APPLIED ORGANOMETALLIC CHEMISTRY, VOL. 7, 253–267 (1993)

Hybrid organosilazane/organosilylamine telechelic oligomers—I. Two-dimensional NMR spectroscopy characterization of dimethylsilylethylenediamine oligomers

Ke Feng, Paul Abrahams and Yitbarek H Mariam
Department of Chemistry, Clark Atlanta University, Atlanta, GA 30314, USA

The detailed characterization of multifunctional hybrid organosilazane/organosilylamine telechelic oligomers by IR and ^{1}H, ^{13}C and ^{29}Si NMR spectroscopy in one and two dimenions has been undertaken. The specific multifunctional oligomers, comprising NH/NH_2 or SiCl functionalities depending on the monomer feed-ratio, were prepared from mono- and di-functionally reacted dichlorodimethylsilane (DDS) and mono-, di-, tri- and tetra-functionally reacted ethylenediamine (EDA). Varying the feed-ratio afforded control of the microstructures of the oligomers and the preparation of oligomers with, in some cases, conterminously located silicon–chlorine (SiCl) groups. The combination of the NMR methods with the IR technique has enabled the detailed microstructural characterization of the oligomers and the identification of the functionalities therein. This approach and the knowledge gained from the DDS/EDA system has been applied to the microstructural characterization of other hybrid organosilazane/silylamine preceramic telechelic oligomers.

Keywords: ^{29}Si NMR characterization, ^{13}C NMR characterization, hybrid organosilazene/organosilylamine, telechelic oligomers, two-dimensional NMR spectroscopy, dimethylsilylethylenediamine, multifunctional

INTRODUCTION

Much research and developmental attention is given nowadays to high-technology ceramics because of their potential uses as engineering and structural materials.[1] However, despite the interest and the progress made in this area,[2–8] the processing technology for high-technology ceramics has not yet reached a stage that would warrant widespread introduction of such materials for various applications.[9] Nevertheless, chemical routes to advanced ceramics[10] have been realized to contribute immensely to the improvement of the processing of ceramics, which is a key technology for the widespread introduction and application of complex materials such as ceramic matrix composites (CMCs).[9] Consequently, great effort has been expended in the design of appropriate precursors that must meet structural and reactivity considerations.[1–8, 11, 12] Furthermore, it is advantageous to control the microstructures of the precursors and the functionalities thereof because it is pertinent to the elucidation of pathways of chain growth, termination and branching.[13] Such mechanistic studies, in turn, can lead to improved synthetic methodologies by, for example, improving yield and shortening reaction times.[13]

One key aspect of the success of the above approaches will depend on knowledge and identification of the microstructures and functional groups of the polymeric precursors, although detailed molecular-level structural elucidation has either been glaringly lacking or inadequate in this area. For example, some solution ^{29}Si NMR data reported on some polysilazanes and related systems had not been very useful because they afforded little insight into the structures/microstructures of the polymers.[14, 15] We were therefore interested in using multinuclear (^{1}H, ^{13}C and ^{29}Si) NMR techniques, including two-dimensional NMR spectroscopy, for the purpose of assessing the utility of such techniques for the elucidation of the microstructures of hybrid carbosilazane/carbosilylamine polymers. Such studies on these hybrid polymers are of interest in their own right because pyrolysis experiments in our laboratories on such systems have shown that some of these systems do give Si–N–C and Si–N–C–O ceramic materials.[16] The work to be reported here specifically deals with the characterization of telechelic

0268-2605/93/040253-15 $12.50

Received 1992
Accepted 29 September 1992

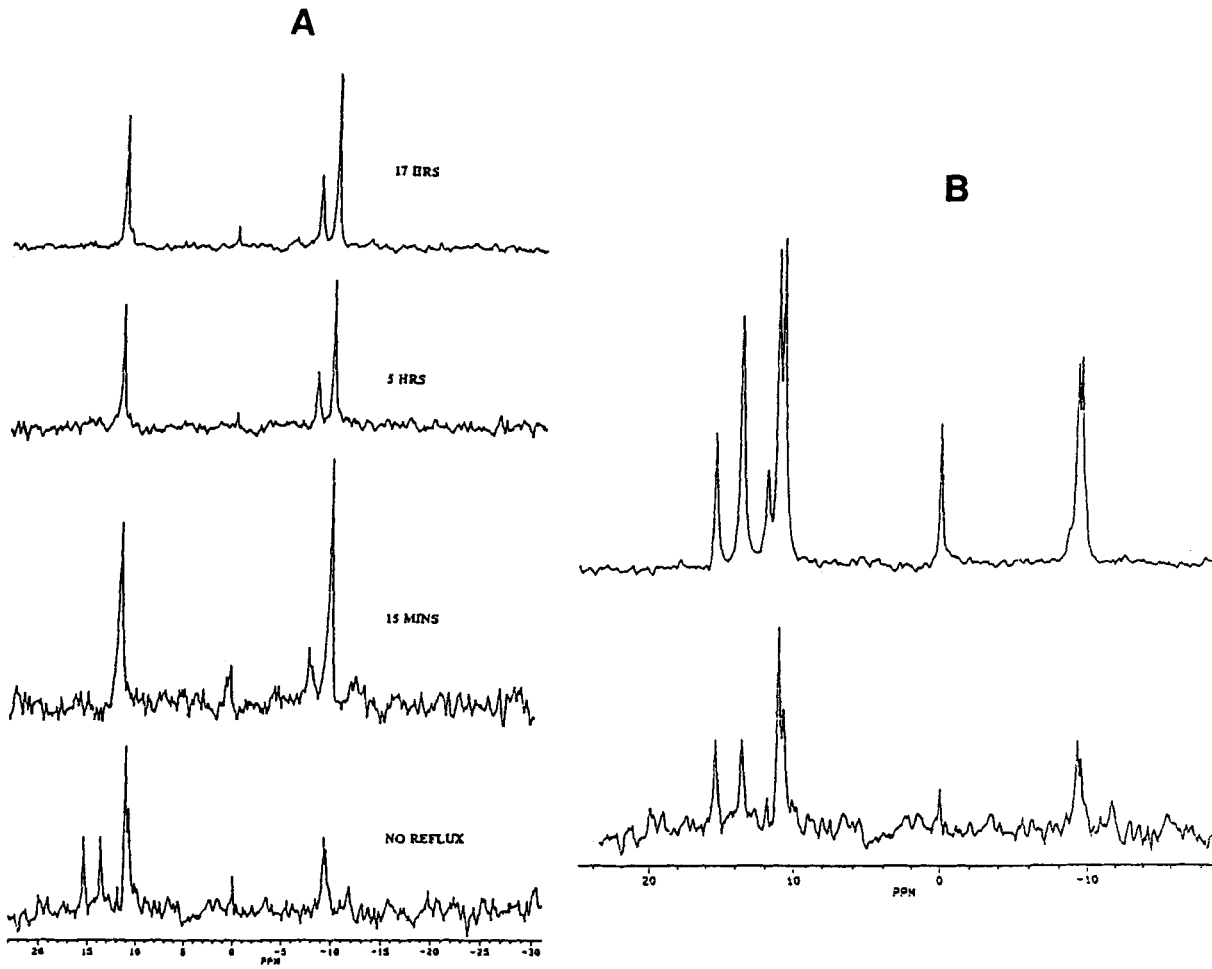

Figure 1 (A) ^{29}Si NMR spectra of PDSED prepared by refluxing the reaction mixture for various periods. Spectra were obtained by the INEPT technique with refocusing for decoupled spectra (INEPTRD). Conditions: pulse sequence, D_1 90° (^{1}H)–D_2 180° (^{1}H), 180° (^{29}Si)–D_2 90° (^{1}H), 90 (^{29}Si)–D_3 180° (^{1}H), 180° (^{29}Si)–D_3–detection with BB in which $D_1 = 4$ s, $D_2 = 0.0416$ s, $D_3 = 0.0208$ s; ^{1}H and ^{29}Si 90° pulse-widths 45 and 24.7 μs respectively, 180° pulse-widths 90 and 49.4 μs, respectively; 16K data points; spectral width 2717 Hz. (B) ^{29}Si NMR spectra of PDSED obtained without refluxing (bottom) and after solution left overnight (top). Conditions were as in A.

oligomeric systems prepared from varying feed-ratios of dimethyldichlorisilane and ethylene-diamine. It demonstrates the utility of the combined use of IR and NMR techniques for unraveling structural information that will be needed to develop further, and expand, the 'database' for precursor chemistry, and specifically, for the detailed characterization of hybrid carbosilazane/carbosilylamine ceramic precursors.

EXPERIMENTAL

Materials

m-Xylene(solvent), ethylenediamine (EDA) and triethylamine (TEA) were all purchased from Aldrich Chemical Co., whilst dichlorodimethyl-silane (DDS) was from Huls America (Petrarch Systems). *m*-Xylene, EDA and TEA were dried

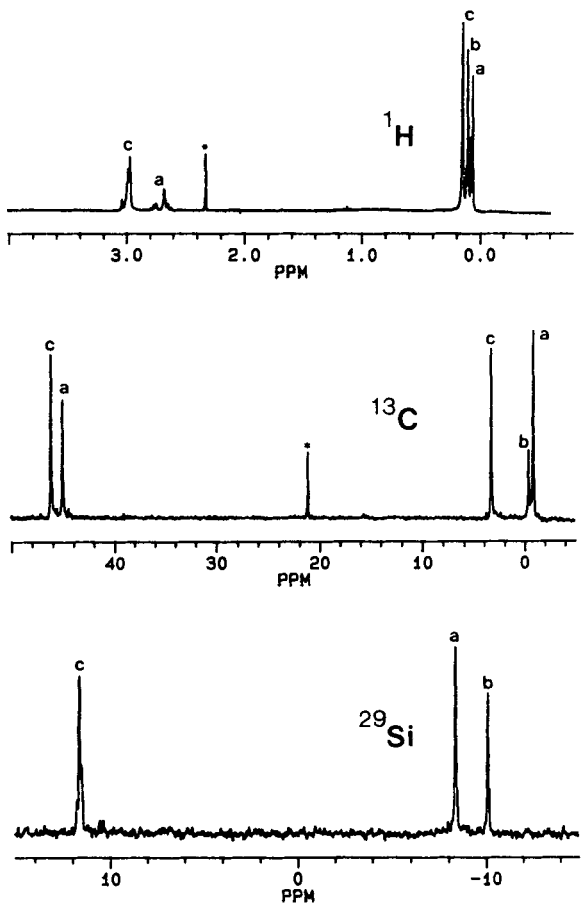

Figure 2 ^{1}H, ^{13}C and ^{29}Si NMR spectra of PDSED (oligomer **II**, $R = 1$). ^{1}H: 8K data points; 6 μs pulse width; eight scans; 4 s relaxation delay. ^{13}C: Broadband decoupled; 8K data points; spectral width 15000 Hz; 20 μs pulse width; 48 scans, 2 s relaxation delay. ^{29}Si: DEPT pulse sequence with recycling time 3 s, spectral width 2500 Hz, delay 0.04 s, 32 scans; 8K data points; observation and decoupling 90° pulse widths were about 23 and 50 μs, respectively. a, b and c refer to acyclic, bridge and cyclic moieties, respectively. The signals indicated by an asterisk are due to solvent (*m*-xylene).

over sodium metal, calcium hydride CaH_2 and P_2O_5, respectively, all under nitrogen and distilled before use. DDS was also distilled under nitrogen before use.

Polymerization reaction

Most oligomers were prepared using varying monomer feed-ratios (R) of DDS:EDA where R varied from 0.67 to 2.5. The amounts of DDS and TEA were always 0.05 and 0.25 mol, respectively, in 10 cm^3 of *m*-xylene whilst the amount of EDA was varied for different R values. The details of the procedure for a prototype polymerization reaction were as reported before.[17]

Analysis and measurement

FTIR spectra were obtained by using a Nicolet 730 system. Thermogravimetric analysis (TGA) was done on a DuPont 951 TGA system interfaced with a Thermal Analysis 2000 unit. NMR spectra were obtained by using a Bruker WM/250 spectrometer. All NMR samples were prepared in a glovebox which contained a dish of P_2O_5 powder and which was maintained under a nitrogen atmosphere. All NMR tubes were oven-dried and evacuated before use. Samples for two-dimensional experiments were contained in sealed NMR tubes. ^{13}C and ^{29}Si spectra were obtained by using primarily the DEPT technique,[18] but the INEPT technique with refocusing for decoupled spectra (INEPTRD) was also used.[18] Unless specified otherwise, chemical shifts were measured relative to the 2.30 ppm methyl resonance of *m*-xylene (internal), the 76.9 ppm resonance of $CDCl_3$ (internal) and TMS (external) for ^{1}H(250.133 MHz), ^{13}C(62.89 MHz) and ^{29}Si(49.69 MHz) NMR experiments, respect-

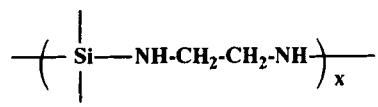

Putative Structure

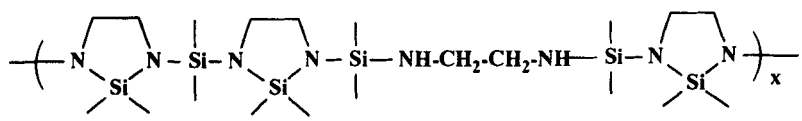

Average Proposed Structure

Figure 3 Proposed structure of PDSED.

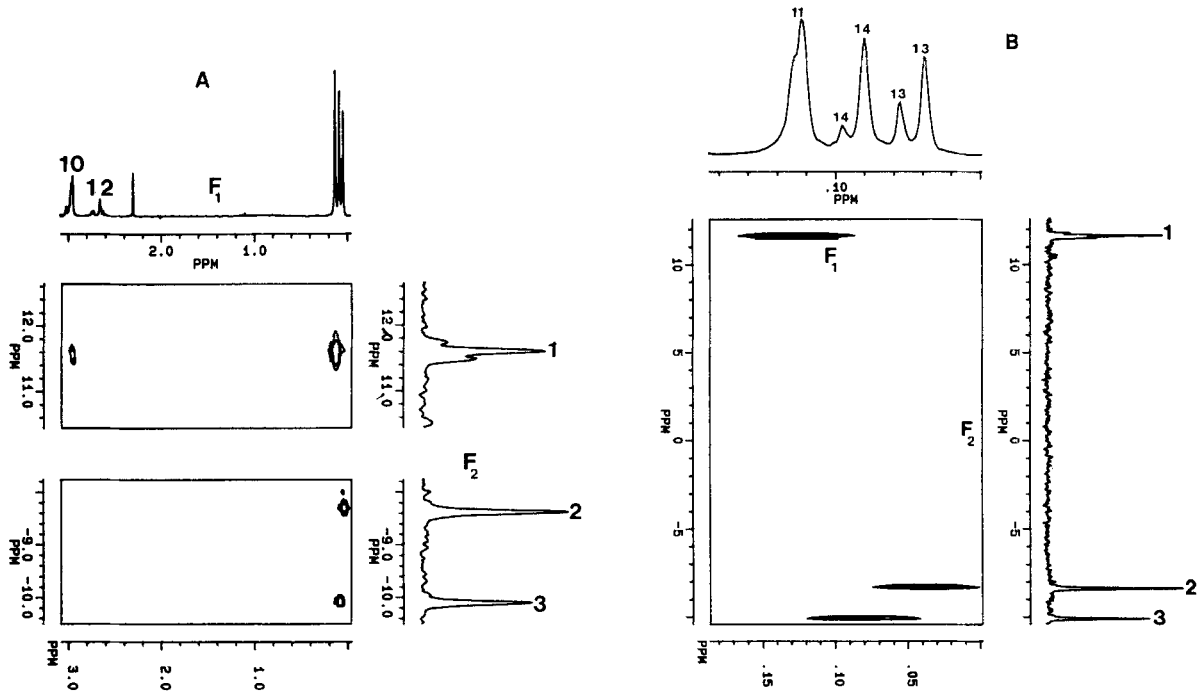

Figure 4 (A) ^{29}Si–^{1}H two-dimensional correlated NMR spectrum for oligomer **II**, $R=1$. Conditions: pulse sequence, D_1 90° (^{1}H)–D_0 180° (^{29}Si)–D_0–D_3 90° (^{1}H), 90° (^{29}Si)–D_4–detection with $D_0=3\,\mu s$, $D_1=3\,s$, and D_3 and D_4 being 65 and 32.5 ms, respectively; $F_1=\pm500$ Hz; $F_2=2000$ Hz; 40 scans (accumulated over $128t_1$ increments); LB = 2 (F_2 dimension only); data matrix = 1024 × 128 (with one level of zero-filling in the F_1 dimension during processing). Magnitude spectra were obtained with the sine bell window function applied in both dimensions prior to FT. (B) Expanded two-dimensional plot showing expansion of the ^{1}H methyl region. The F_1-dimension signals in this and all other two-dimensional plots should be indicated by a number and a prime (which has been omitted in most cases). The correlations show: signals **10′** (^{1}H, methylene, 3 ppm) and **1** (^{29}Si) are for cyclic structures (Fig. 3A); signal **11′** (0.12 ppm) which correlates with **1** (^{29}Si) is due to ring methyl; likewise, signals **14′** (^{1}H, 0.08 ppm) and **3** (^{29}Si) signify bridge; and signals **13′** (^{1}H, 0.03 ppm) and **2** (^{29}Si) are acyclic.

ively. Most two-dimensional COSY spectra were obtained by using standard techniques;[19–21] ^{13}C–^{1}H two-dimensional COSY spectra were obtained by using the homonuclear broad-band decoupled shift correlation NMR method.[22]

Effect of hydrolysis on ^{29}Si NMR spectra

Since the oligomers were found to be sensitive to trace amounts of water or moisture, the ^{29}Si spectra of all samples were compared with ^{29}Si spectra obtained by intentionally adding some water to a sample to assure that hydrolysis has not occurred. All samples for two-dimensional experiments were checked in this way before and after the experiments. If any hydrolysis was detected, the data were discarded.

RESULTS AND DISCUSSION

Initial ^{29}Si NMR studies

As exploratory studies of structural changes during reaction time, a reaction between DDS and EDA (1:2 ratio, respectively) in toluene was carried out for various refluxing periods and the ^{29}Si spectra obtained are shown in Fig. 1. It is clear that the spectrum for zero reflux time (no reflux) is markedly different from the others (Fig. 1A); it is also evident that there is hardly any difference between the spectra for short and long refluxing periods. Interestingly, comparison of the spectra in Fig. 1(B) shows significant changes in intensities. Both increments and decrements in intensity are observed, suggesting that one type of structure is being converted to some other type. These spectra gave some clues that the micros-

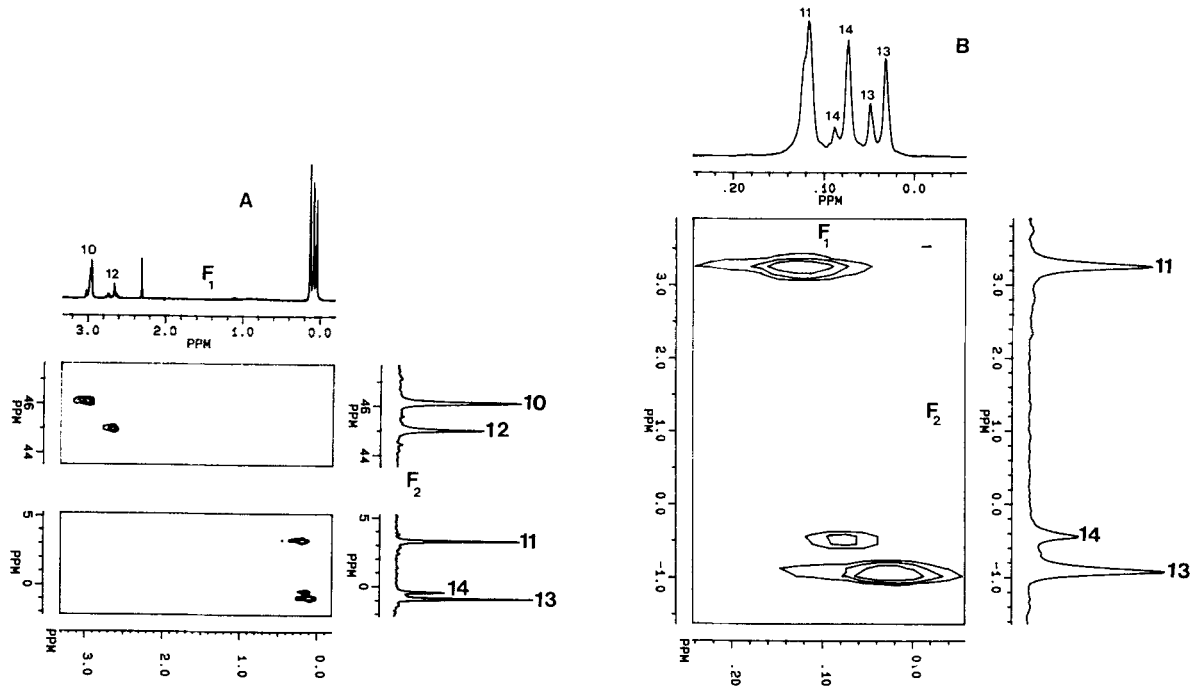

Figure 5 (A) Broadband homonuclear decoupled ^{13}C–^{1}H two-dimensional correlated NMR spectrum of oligomer **II**, $R=1$. Conditions: pulse sequence, D_1 90° (^{1}H)–D_0 90° (^{1}H)–D_3 180° (^{1}H), 180° (^{13}C)–D_3 90° (^{1}H)–D_0–D_3 90° (^{1}H), 90° (^{13}C)–D_4–BB, FID with $D_0=3\,\mu s$, $D_1=3\,s$, and D_3 and D_4 being 4.1 and 2.05 ms, respectively; $F_1=\pm 600$ Hz; $F_2=3500$ Hz; 24 scans; other conditions as in Fig. 4. (B) Expanded two-dimensional plot showing expansion of the methyl regions. ^{13}C assignments are: cyclic and acyclic —CH_2CH_2— at 46.13 and 44.98 ppm (signals **10** and **12**), respectively, ring, bridge and acyclic CH_3— groups at 3.25, −0.49 and −0.97 ppm (signals **11**, **14** and **13**), respectively.

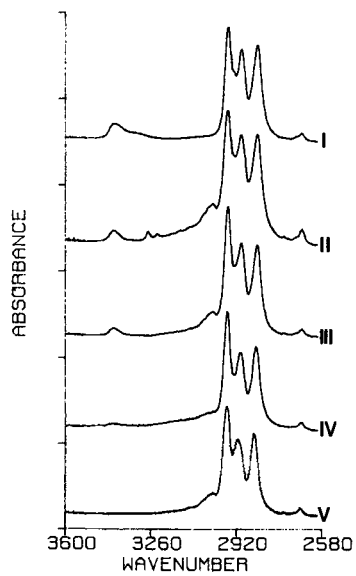

Figure 6 2580–3600 cm^{-1} region of the IR spectra of the various oligomers. R values for **I–V** are 0.67, 1, 1.33, 1.82 and 2, respectively.

tructure and/or the nature of the functional groups in these systems might be controllable to some degree. Also, since not much ^{29}Si NMR work has been done on these systems, the results were interesting enough to warrant the detailed structural elucidation studies described here.

Characterization of oligomer II, $R=1$

The ^{1}H, ^{13}C and ^{29}Si NMR spectra of poly(dimethylsilylethylenediamine) (PDSED) prepared from a 1:1 molar ratio of dimethyldichlorosilane and ethylenediamine (and 5 parts of triethylamine) are shown in Fig. 2. The early ^{1}H NMR work by Kummer and Rochow,[23] who used a 1:2 ratio without TEA, and recently confirmed by us by multinuclear NMR characterization,[16,17,24] indicated that the polymer contained a significant fraction of cyclic structures. Figure 3 shows two structures of PDSED. Of these, the putative structure will be predicted to form from simple condensation of the monomers. The other one, labelled 'Average proposed structure', represents the experimentally observed cyclic and acyclic composition (about 70% cyclic for

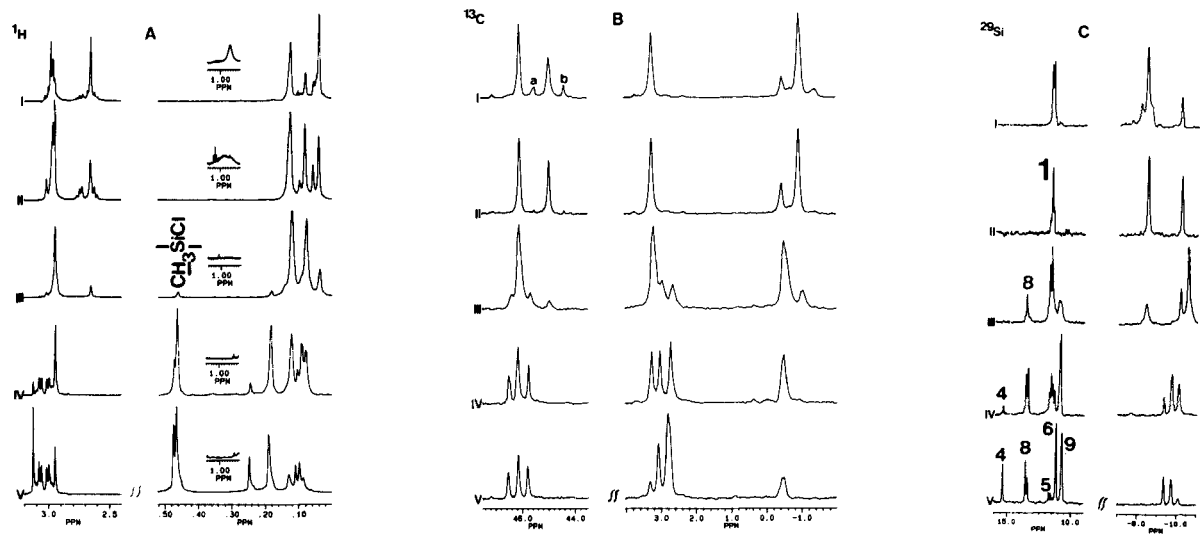

Figure 7 NMR spectra of oligomers I–V. (A) ^{1}H; R values as in Fig. 6; conditions as in Fig. 2 (^{1}H). (B) ^{13}C; conditions as in Fig. 2 (^{13}C). The assignments of signals a and b are discussed in Table 1. (C) ^{29}Si; number of scans varied from 32 to 96; observation 90° pulse width, 22–24 μs; decoupling 90° pulse width, 48–52 μs; conditions as in Fig. 2 (^{29}Si).

the 1:1 ratio) and one of the possible sequences. The NMR spectra in Fig. 2 are consistent with this proposed structure (*vide infra*) and not with the putative one.

The strategy used for the detailed NMR characterization of PDSED oligomers prepared with different R values was to establish connectivities (via two-dimensional COSY NMR) with proton signals that have already been assigned definitively and to use the ^{29}Si–^{1}H and ^{13}C–^{1}H correlations to make further detailed assignments. Since the ^{1}H NMR work of Kummer and Rochow[23] on model compounds showed that the cyclic and acyclic —CH_2CH_2— proton signals appear at 3 and 2.65 ppm respectively, this information was, by and large, adequate to make all other assignments using connectivities that arose from the two-dimensional COSY experiments. Figure 4 shows correlation between the proton signal at 3.0 ppm (**10′**) and the ^{29}Si signal at 11.6 ppm (**1**). Since the former has been assigned as cyclic by Kummer and Rochow,[23] the assignment of the cyclic ^{29}Si signal is thus confirmed. (In the numbering scheme in the figures, the primes for the proton signals have been omitted.) The acyclic —CH_2CH_2— signals at 2.65 ppm (**12′**) should correlate with the ^{29}Si signal at −8.46 ppm (**2**) but this is not observed in Fig. 4, presumably because of lack of sensitivity under the experimental conditions used. The correlation was confirmed, however, in a two-dimensional experiment using oligomer **I** ($R = 0.67$, not shown). Other assignments are indicated in the Figure. The assignment of the most downfield ^{29}Si signal to the azasilacyclopentane is consistent with the expected dependence of ^{29}Si chemical shifts on bond strain. Furthermore, Cragg and Ma[25] had shown that for a model compound they synthesized, bis(1,3,2-diazasilacycloalkyl)dimethylsilane, the ring silicon atoms and the silicon in the bridge dimethylsilyl group (between cyclic moieties) appeared at 10.63 and −9.51 ppm, respectively. We have also obtained the ^{29}Si NMR spectrum of the commercially available bis(monoethylamino)dimethylsilane, which has a chemical shift of −8.6 ppm, i.e. very similar to that of the acyclic moiety. The above assignments from the two-dimensional experiments are thus consistent with these findings.

Using the known assignments of the proton spectrum and the correlations observed in the two-dimensional ^{13}C–^{1}H correlated spectra in Fig. 5, assignments of the ^{13}C signals can be made (indicated in the Figure).

Spectra of oligomers prepared from varying monomer feed-ratios (*R*)

Figure 6 shows the functional region of the IR spectra of PDSED prepared from the various ratios (R) indicated in the Figure. No NH or NH_2 is observed for oligomer **V**; oligomers **III** and **IV** show NH (3406 cm^{-1}); both NH and NH_2

(3315 cm^{-1}) are however observed for oligomers **I** and **II**.

Figure 7(A)–(C) shows the ^{1}H, ^{13}C and ^{29}Si NMR spectra of the oligomers. It is clear that the spectra for oligomers **IV** and **V** show the greatest changes. The proton signals at 0.47 and 0.48 ppm can be assigned to CH_3Si—Cl. This assignment is consistent with the electron-withdrawing effect of the Cl atom; reacting an oligomer of this ratio with EDA or NH_3 results in the disappearance of the proton signals, thus providing additional supporting evidence for a silicon–chlorine (Si–Cl) functionality. The ^{29}Si signal at about 13.5 ppm (**8** in Fig. 7) is downfield from the cyclic ^{29}Si signal at 11.6 ppm (**1** in Fig. 7). Signal **8** therefore probably arises as a result of the perturbation of the electronic structure and/or geometry of the ring system by the Si–Cl functionality. This is more evident in the spectra for oligomers **IV** and **V** which contain more Si–Cl functionality.

Chemical shifts, assignments and ^{29}Si–^{1}H and ^{13}C–^{1}H correlations

The ^{29}Si, ^{13}C and ^{1}H chemical shifts of the various NMR signals observed for the different oligomers are summarized in Table 1. The signals are identified by the type of moiety (ring, acyclic or bridge) and functionality they represent. Although some of the experimental evidence used to extract this Table is to be presented later (*vide infra*), the Table is presented here to aid in the discussion of the two-dimensional NMR data. The entries in the Table are designed to show the correlation and/or connectivities observed in the two-dimensional NMR experiments (see Table 1 for details). When used in conjunction with Fig. 9

Table 1 ^{1}H, ^{13}C, ^{29}Si chemical shifts and assignments

	^{29}Si		^{1}H[a]		^{13}C[a]		
Moiety	agn[e]	cs[e]	agn	cs	agn	cs	Segment[b,d] (Fig. 9)
Ring	**1**	11.6	**10′**	2.91–3.02[c]	**10**	46.13[c]	**A**
			11′	0.12	**11**	3.25	
Acyclic	**2**	−8.46	**12′**	2.59, 2.75[c]	**12**	44.98[c]	**B**
			13′	0.03, 0.06	**13**	−0.97	
Bridge	**3**	−10.12	**14′**	0.08, 0.10	**14**	−0.49	**A**
					a	45.39[c]	**F**
					b	44.19[c]	
Ring	**4**	15.33	**15′**	3.14[c]	**15**	46.16[c]	**C**
			16′	0.25	**16**	2.85	
Ring	**5**	11.40, 11.80	**17′**	0.13	**17**	3.33	
Functional	**6**	11.15	**18′**	0.48	**18**	2.78	
Bridge	**7**	−9.36	**19′**	0.07–0.12	**19**	−0.49	
	7*	−9.75					
			20′	3.01, 3.03[c]	**20**	45.77[c]	**D**
Ring	**8**	13.53, 13.58	**21′**	0.19	**21**	3.1	
Functional	**9**	10.7	**22′**	0.47	**22**	2.75	
			c′	3.07, 3.09[c]	**c**	46.53[c]	

[a] ^{13}C signals **a**, **b** (Fig. 7B), **c** and **20** (Fig. 10C), and ^{1}H signals **c′** and **20′** (Fig. 10C) have not been assigned definitively, but **a** and **b** are probably due to segment **F** (Fig. 9), and the tentative assignments of **c** and **20**, as well as that of **c′** and **20′**, are probably interchangeable. [b] The last column assigns the segment to which a given moiety or functional group belongs. For example, the first entry is for a ring moiety in segment **A** (Fig. 9) with signals **1** (^{29}Si), **10** and **11** (^{13}C), and **10′** and **11′** (^{1}H). The first entry is also designed to show the ^{29}Si–^{1}H correlation of Si atom **1** with methylene protons **10′** and with methyl protons **11′**, as well as the ^{13}C–^{1}H correlations between methylene protons **10′** and carbons **10**, and between protons **11′** and carbon **11** of the methyl group. [c] Chemical shifts are for methylene protons and carbons; all other ^{1}H and ^{13}C chemical shifts are due to methyl groups. [d] Only Si and C atoms are indicated by numbers in Fig.9; an H atom attached to a given C atom is indicated by the number of that C atom with a prime. [e] agn and cs denote assignment and chemical shift (ppm), respectively.

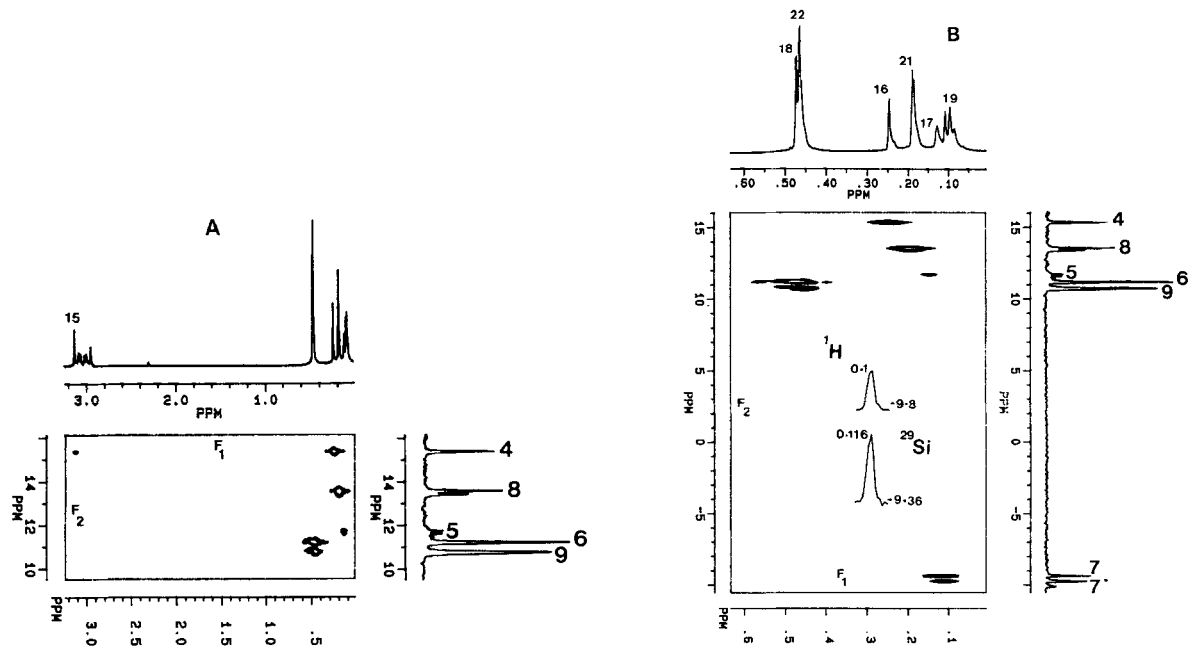

Figure 8 A ^{29}Si–^{1}H two-dimensional correlated spectrum of oligomer **V**. Conditions as in Fig. 4 with 24 scans, $D_3 = 70$ ms, $D_4 = 35$ ms. Note the correlation between **15′** and **4**. (B) Expanded two-dimensional plot. Inset shows cross-sections parallel to the F_2 axis at the ^{29}Si chemical shifts of the projection peaks **7** (−9.36 ppm) and **7*** (−9.8 ppm). Correlations observed are between: **18′** and **6**; **22′** and **9**; **16′** and **4**; **21′** and **8**; **17′** and **5**; **19′** and **7** (also **7***).

and Scheme 1 and the various spectra, Table 1 summarizes the assignments made.

Two-dimensional COSY spectra of oligomer V

The ^{29}Si–^{1}H two-dimensional COSY spectra of oligomer **V** are shown in Fig. 8. The proton signals at 0.48 and 0.47 ppm (**18′** and **22′**, respectively, in Fig. 8B) have been assigned to $\underline{CH_3}$ Si–Cl and their correlations with the ^{29}Si signals **6** and **9** allow the assignment of the ^{29}Si signals to $\underline{Si}$–Cl. ^{29}Si signals **4** and **8** are downfield from signal **5** (or **1** in Figs 4 and 7), which is due to the azasilacyclopentane moiety. Since these signals do not correlate with the protons of $\underline{CH_3}SiCl$, they cannot be due to the Si–Cl functionality. Nor could they be due to acyclic or bridge moieties because the chemical shift difference between signals **4** and **8**, and signals for the acyclic and bridge moieties (upfield region of spectrum) is so large that it cannot be accounted for by microstructural changes and/or effects due to functional groups, suggesting that the signals are probably due to ring moieties. Upon closer examination of the ^{29}Si NMR spectra in Figs 7, 8 (and 12), it is evident that the intensities of **4** and **6**, and the intensities of **8** and **9**, increase or decrease concomittantly, i.e. the signals in each pair must be associated with each other structurally. Hence, **4** and **8** must be due to ring moieties adjacent to an Si–Cl functionality and are assigned to atoms **4** and **8** in segments **C** (or **C***) and **D** (Fig. 9), respectively. Segment **C*** is simply a combination of segments **C** and **E**, and Si atom **5** is assigned a chemical shift that is very similar to that of **1** in segment **A**. It should be noted here that the spectrum in Fig. 1 (bottom, no reflux) is very similar to that of oligomer **V**. Having elucidated the structure of oligomer **V**, it is clear that a reaction when $R = 0.5$ (with no TEA added) gives some Si–Cl and a long period of refluxing is not apparently necessary to react further the Si–Cl functionalities. The results may suggest that the major pathway of the polymerization reaction between DDS and EDA probably proceeds via branching and then cyclization (*vida infra*).

The ^{13}C–^{1}H two-dimensional COSY spectra are also given in Fig. 10. In this case the resolution is not as good for detailed assignments. For example, detailed analysis showed correlations between ^{1}H signals **18′** or **22′** and the ^{13}C signals at 2.75 and 2.78 ppm (**18** and **22**) and ^{1}H signal (**16′**) at 0.25 ppm and the ^{13}C signal at 2.85 ppm (**16**)

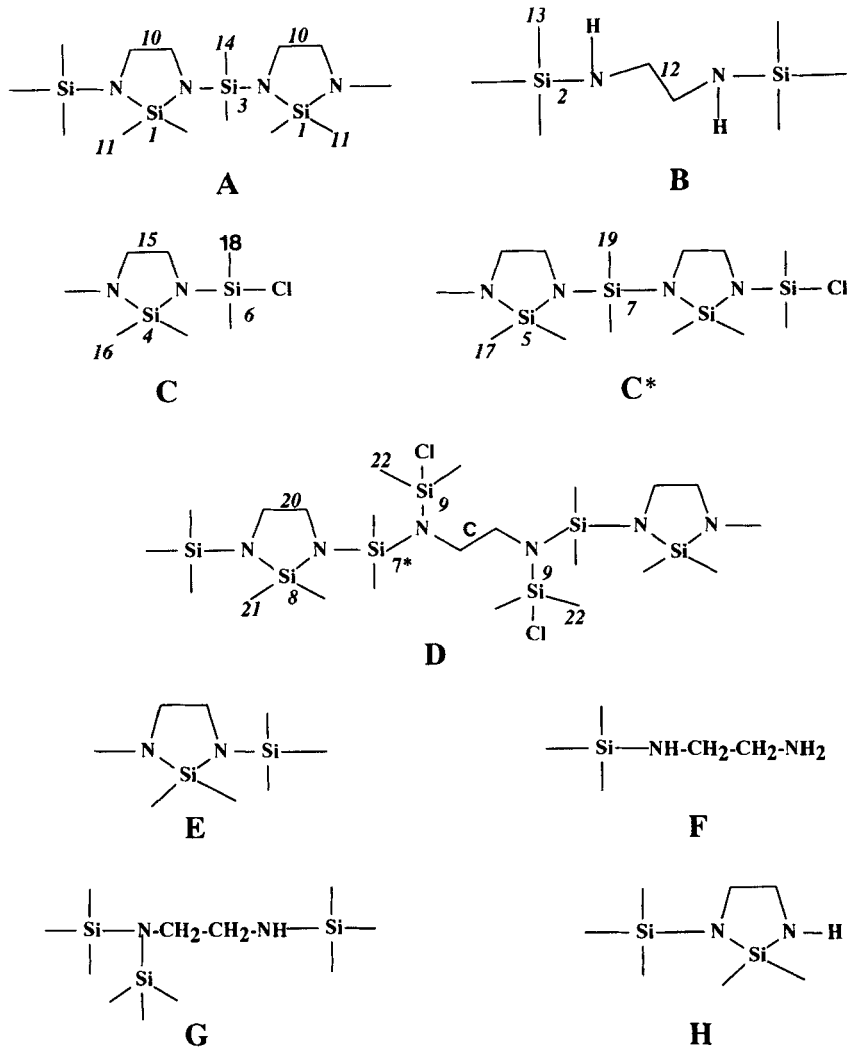

Figure 9 Possible/proposed functional groups and backbone compositions.

(Fig. 10B). These correlations were gleaned from analysis of two-dimensional slices since the ^{13}C signals (**16**, **18** and **22**) apparently overlap (Fig. 11). Other correlations observed are indicated in Fig. 10 (B, C).

Functional groups and backbone composition

The variations in backbone structure and functional group with *R* can be accounted for, by and large, by a combination of the structural segments shown in Fig. 9 and Scheme 1, and the composition for each *R* value is summarized in Table 2. For example, oligomer **II** has primarily a composition of 69% cyclic structures and can be represented by segments **A** and **B** (Fig. 9). Oligomer **I** is similar to **II** but has only 50% cyclic structures and thus contains more of segment **B**. As a result, it can be expected to have a greater fraction of segment **E** (isolated rings). That this is so is evident in the proton spectra in Fig. 7(A) and the data in Table 2 which show the relative intensities of signals **11′** (ring), **14′** (bridge) and **13′** (acyclic). Other segments that are probably present but in small amounts are also indicated in Table 2. Similarly, as can be seen in the ^{1}H spectra in Fig. 7(A), the predominant segment in oligomer **III** is **A** and other minor segments are indicated in Table 2. Oligomers **IV** and **V** contain the Si—Cl functionality which shifts the acyclic —CH_2CH_2— ^{1}H signals downfield to the region where the cyclic

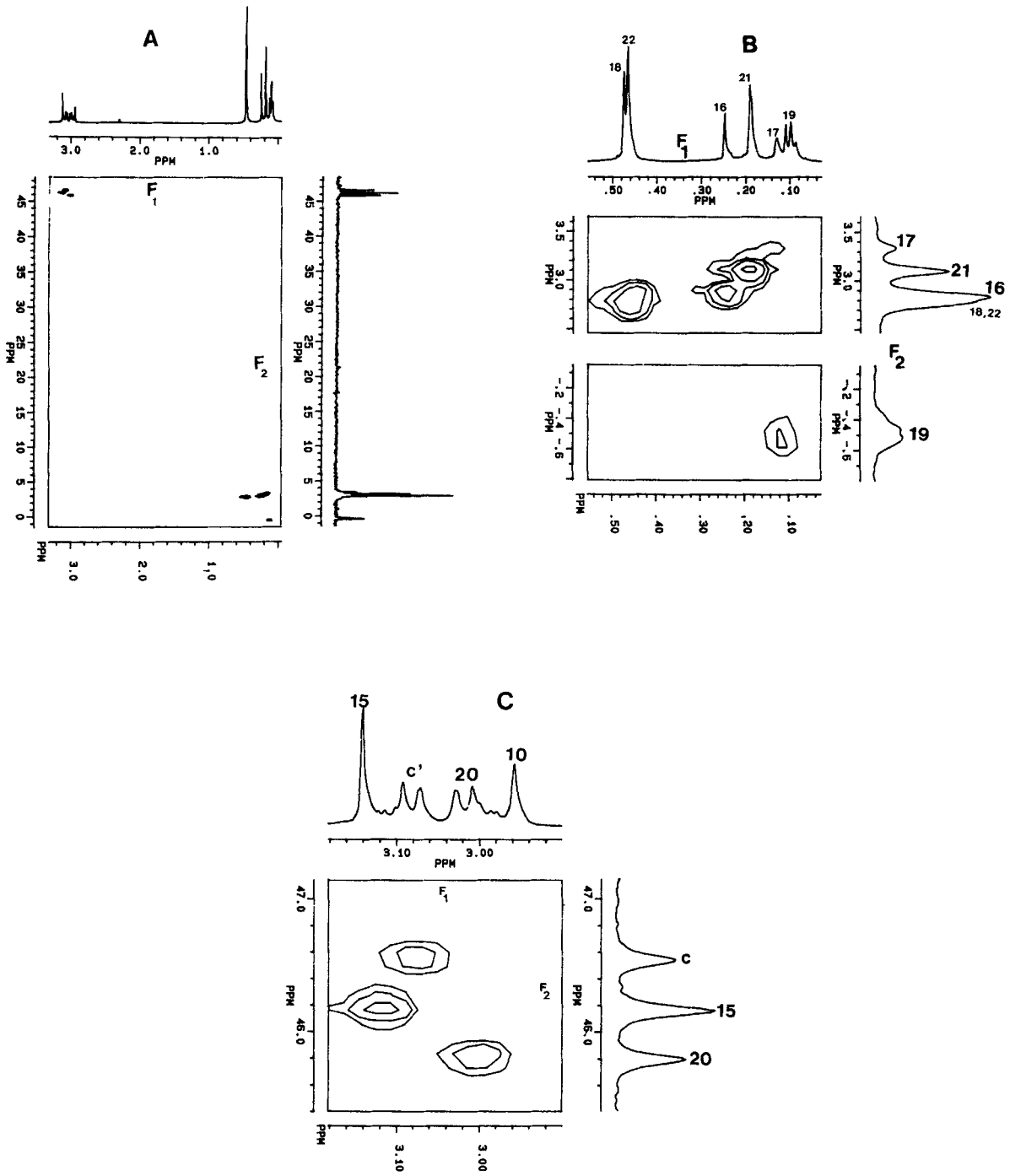

Figure 10 (A) ^{13}C–^{1}H two-dimensional correlated spectrum of oligomer **V**. Conditions as in Fig. 5 with 32 scans. (B) Two-dimensional plots showing expansion in the methyl region. Correlations not discussed in the text are between: **17′** and **17**; **19′** and **19**; **21′** and **21** (in the F_1 and F_2 dimensions respectively). (C) Two-dimensional plots showing expansion in the methylene region. Correlations observed are between: **10′** and **15**; **15′** and **15**; **20′** and **20**; **c′** and **c** (in the F_1 and F_2 dimensions, respectively).

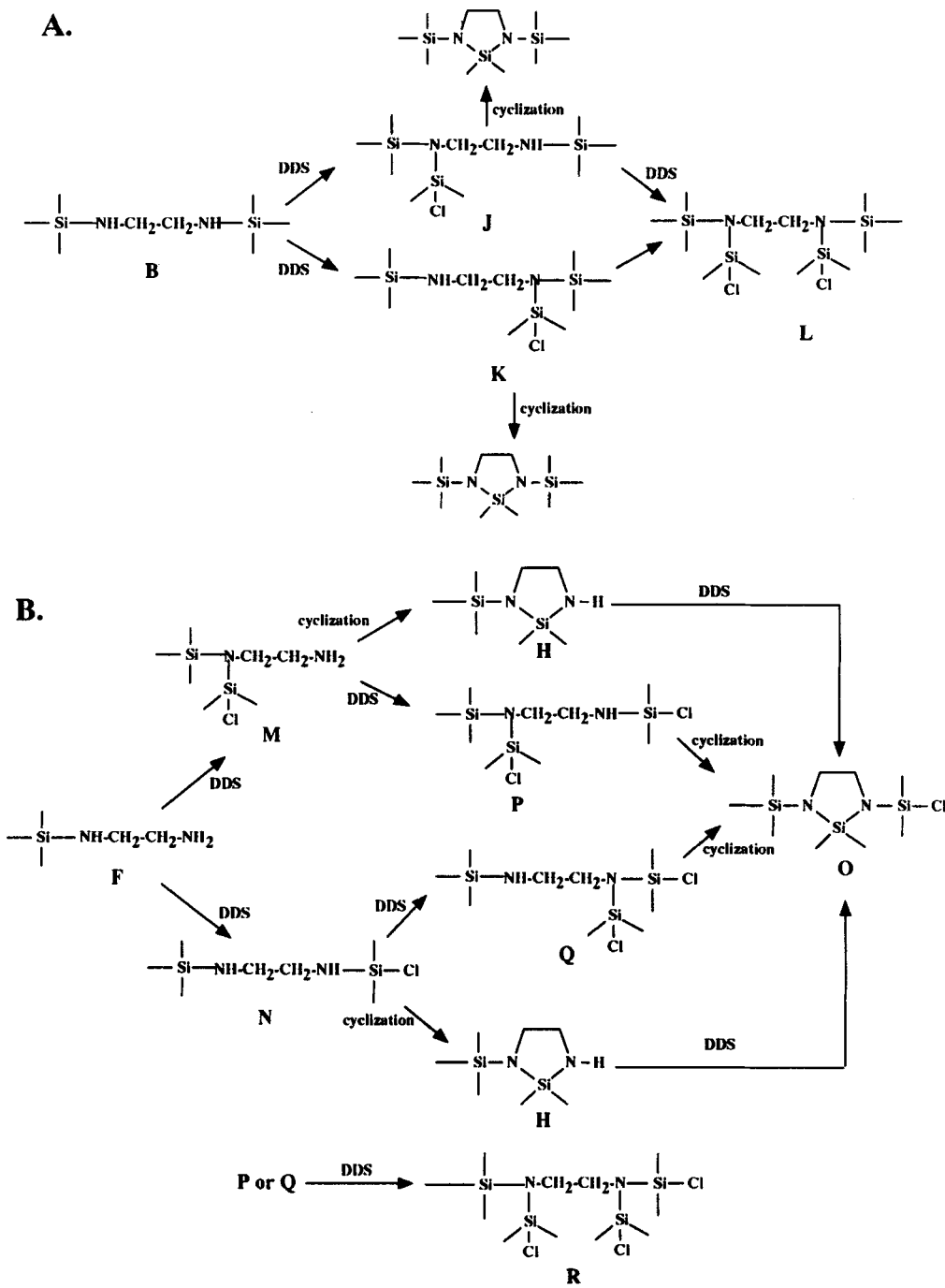

Scheme 1 Proposed reactions during the postpolymerization modification of oligomer **II** with DDS.

—CH_2CH_2— appear. It was not therefore possible to calculate the cyclic: acyclic ratio for these oligomers using the methylene region. Judging from the intensity of ^{29}Si signal **5** [Figs 7(C) and 8], however, these oligomers should contain some amounts of segments **A** and/or **E**, and predomi-

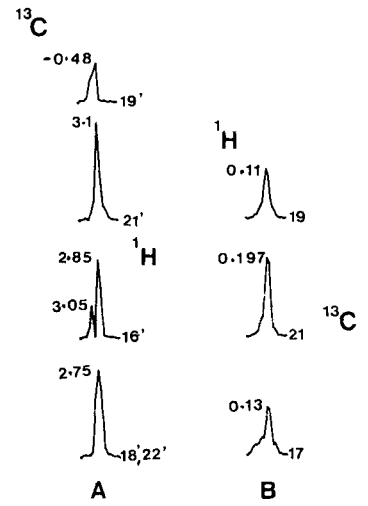

Figure 11 Cross-sections parallel to the F_1 (A) or F_2 (B) axes at the ^1H (A) or ^{13}C (B) chemical shifts of the projection peaks, respectively. The data present supporting evidence for the connectivities summarized in Table 1, where the chemical shifts of the ^{13}C and ^1H projection peaks are listed.

nantly segments **C** and **D**. Further discussion rationalizing why oligomers **IV** and **V** should have segments **C** and **D** is provided in the next section.

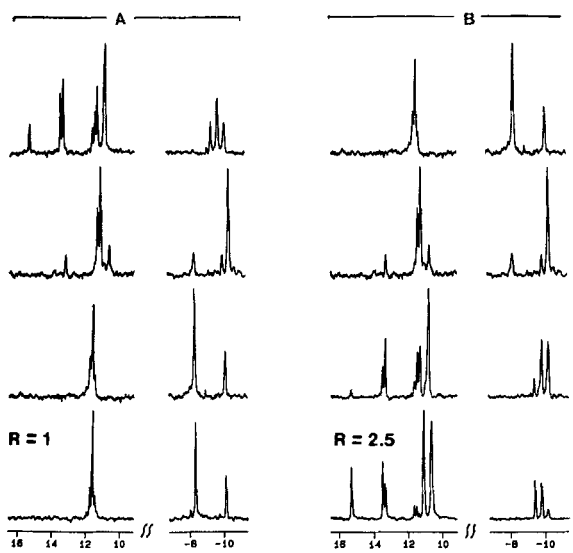

Figure 12 ^{29}Si NMR sets of spectra obtained by the inverse-gated decoupling technique with recycling time 90 s, spectral width 5000 Hz, 8K data points, pulse width 20 μs, 40–120 scans (see text for reaction details). $R = 1$ for set A, bottom spectrum and $R = 2.5$ for set B, bottom spectrum.

Potential for postpolymerization modification: stepwise reaction

The oligomers prepared with various R values should be useful for postpolymerization modifications as a means of controlling the microstructure and the composition of the oligomers. This, for example, can be accomplished by starting with a certain monomer feed-ratio R, and reacting the resulting oligomer with the appropriate monomer (in a stepwise manner). Figure 12 illustrates two such cases. The bottom spectrum in Figure 12(A) is for the starting oligomer ($R = 1$). When this oligomer (with —NH and some —NH_2 functionality) is reacted (stepwise) with DDS, the backbone structure and the functional groups of the resulting oligomer, as can be gleaned from the spectra, resemble that shown in Fig. 7(C) (for oligomer **V**). Figure 12(B) shows the results obtained when a starting oligomer of $R = 2.5$ is reacted (stepwise) with EDA. The microstructure of the final oligomer in this case resembles that shown in Fig. 7(A) (for oligomer **II**). It is thus evident from the data in Fig. 12 that an oligomer akin in structure to that for $R = 1$ can be converted to an oligomer with structure akin to that for $R = 2.5$, and vice versa.

The modification of the preformed $R = 1$ oligomer by stepwise addition of DDS helps to elucidate the microstructure of oligomer **V**. The microstructure of the $R = 1$ oligomer, **II**, has already been elucidated and it contains primarily segments **A** and **B**, and some **E**, **F** and **G** (Fig. 9). Of these, only the —NH functionalities of **B** and **F** can react with DDS as shown in Scheme 1. When there is a sufficient excess of DDS (as is the case for $R = 2.5$), one can easily envisage how a segment like **B** can be converted to a segment like **D** (cf. segment **L** Scheme 1) and how **F** can be converted to **O** (cf. segment **C**, Fig. 9). Since there is no —NH or —NH_2 functionality in oligomer **V**, segments **F** and **G** in Fig. 9 and segments **K**, **M**, **N**, **P** and **Q** in Scheme 1 can be ruled out as constituents of oligomer **V**. The ^{29}Si NMR spectra for oligomer **V** (Fig. 7C) and oligomer **II** after modification with DDS (Fig. 12A) are similar except for differences in signal intensity, and the foregoing discussion rationalizes how segments such as **C** and **D** can be obtained from oligomer **II**. With the IR and NMR data taken as a whole, as well as the supporting information gleaned from the stepwise reaction (Fig. 12A), we conclude that oligomer **V** contains predominantly combinations of segments **C** and **D**.

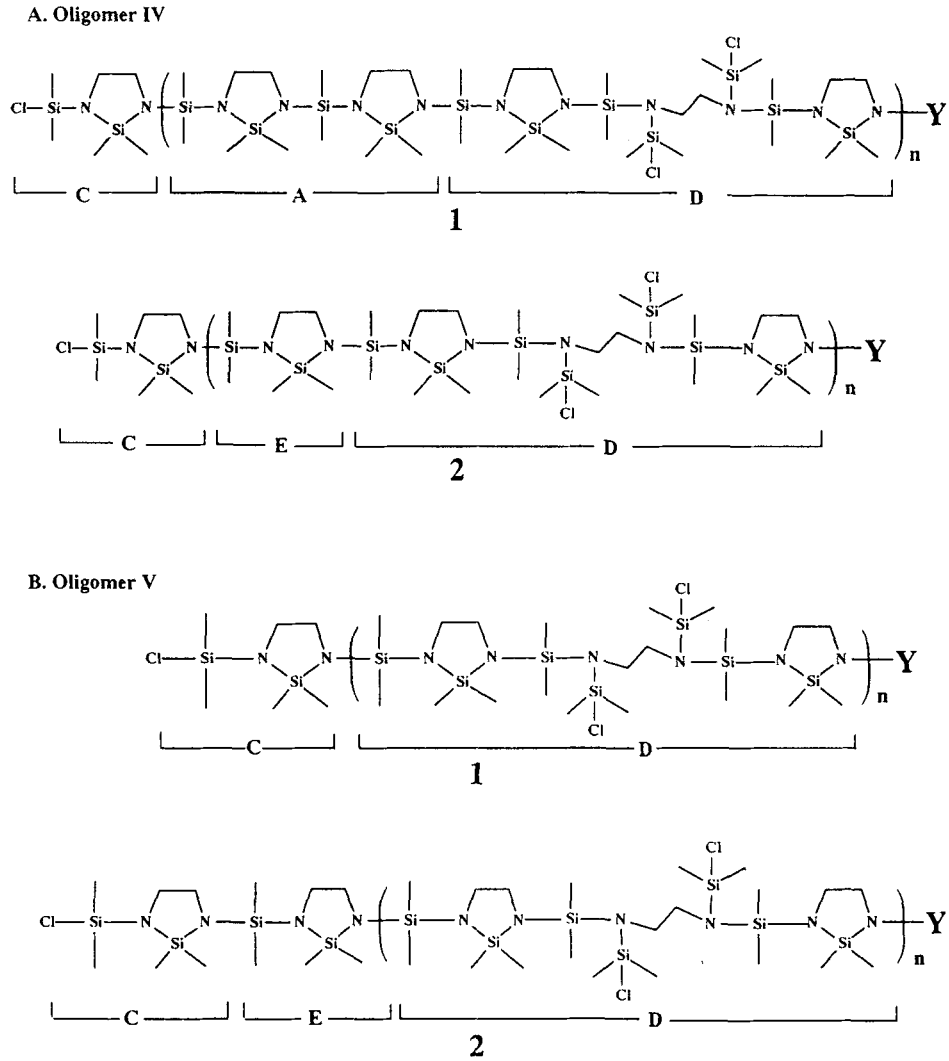

Figure 13 Examples of possible/proposed 'average' structures for oligomers **IV** and **V**, i.e. the most likely structures consistent with ^{1}H NMR signal intensity data. Y represents unspecified end groups such as **C** (Fig. 9) or possibly **R** (Scheme 1B), or SiCl.

Proposed structures

The data presented, when taken in totality, should enable one to propose representative structures for the oligomers by taking combinations of segments and functional groups presented in Fig. 9 and Scheme 1, although the exact sequence of segments and positions of the functional groups cannot be ascertained from the data. The proposed structure of oligomer **II**, given in Fig. 3, can for example be constituted by taking one of each of segments **A**, **B** and **E**. Proposed structures are also presented for oligomers **IV** and **V** in Fig. 13. Structures **A,1** and **B,1** are proposed to be major forms of oligomers **IV** and **V**, respectively; structures similar to **A,2** and **B,2** (Fig. 13) must be present, however, to account for most of the data presented.

CONCLUSION

The system investigated in this work has served to illustrate that a rather simple approach which involves controlled conventional condensation

Table 2 Summary of backbone composition and functional groups of each oligomer
(A) Backbone compositions

	Composition							
	Major/minor[a]					Some[b]		
Oligomer	A	B	C	D	E	F	G	H
I	+	++	—	—	++	+	+	?c
II	+++	++	—	—	+	+	+	?c
III	+++	+	—	+	+	+	+	?c
IV	+	—	++	++	+	—	—	—
V	—[d]	—	+++	+++	+	—	—	—

[a] Entries with more pluses represent major components. [b] Relatively small to minimal. Larger than 5-membered ring moieties may also be present. [c] Proposed to be present but not experimentally confirmed. [d] — Not present.

(B) Functional groups and other relevant data

		Functional group				
Oligomer	Cyclic (%)[a]	NH	NH_2	SiCl	Cl (%)[b]	Compositional ratio[c]
I	50	++	+	—	0	0.9:0.4:1
II	69	++	+	—	0	0.6:0.6:1
III	89	+	—	+	2	0.2:0.8:1
IV	?[d]	+	—	++	24	0.7:1[e]
V	?[d]	—[f]	—	+++	39	0.4:1[e]

[a] Determined from ^1H signal integration of the methylene region. [b] Estimated from integration of ^1H signals **18'** and **22'**. [c] Determined from integration of the methyl region of the spectra in Fig. 7; ratios correspond to groups of signals that correspond to the ratio acyclic (**13'**):bridge (**14'**):ring (**11'**). [d] Not determinable. [e] Ratio corresponds to (acyclic + bridge):ring. [f] — Not present.

reactions can be available for the synthesis of ceramic precursors and for the development of a 'database' for precursor chemistry. Our approach has been,[26] and is being, extended to systems that can serve as ceramic precursors. The data reported here also illustrate that a combination of IR and ^{29}Si, ^{13}C and ^1H NMR techniques can be extremely valuable for unravelling structural information in hybrid organosilazane/silylamine systems, information that will certainly be needed to expand the 'database' for precursor chemistry.

Acknowledgement We are grateful for the financial support of this work by DOE/BES Grant No DE-FG05-87ER45306. This work has also benefited from the partial financial support for the upgrade of the WM-250 NMR spectrometer by grants from the NSF (RII-8505478), the ONR (N00014-K-0404) and the NIH/RCMI (Grant No RR03062). We also acknowledge financial support from the AFOSR (Grant No AFOSR-87-0123) and the NSF (Grant No RII-8505478) for the acquisition of the TGA/FTIR system.

REFERENCES

1. Segal, D L *Br. Ceramic Trans. J*, 1986, 85: 184
2. Yajima, S, Hasegawa, Y, Okamura, K and Matsuzawa, T *Nature (London)*, 1978, 273: 523
3. Wynne, K J and Rice, R W *Annu. Rev. Mater. Sci.*, 1984, 14: 297
4. Walker, B E Jr, Rice, R W, Becher, P F, Bender, B A and Coblenz, W S *Am. Ceram. Soc. Bull.*, 1983, 62(8): 916
5. Rice, R W *Am. Ceram. Soc. Bull.*, 1983, 62(8): 889
6. Laine, R M, Blum, Y D, Tse, D and Glaser, R In: *Inoranic and Organometallic Polymers*, Zeldin, M, Wynne, K J and Allcock, H R (eds), American Chemical Society, A.C.S. Symp. Ser. No. 360, Washington, D.C., 1988, Chapter 10
7. Baney, R H In: *Ultrastructure Processing of Ceramics, Glasses and Composites.* Hench, L L and Ulrich, D R (eds), John Wiley, New York, 1984, Chapter 20
8. For general references see *Silicon-Based Polymer Science: A Comprehensive Resource*, Ziegler, J M and Gordon

Fearon, F W (eds), A.C.S. Adv. Chem. Ser. No. 224, Washington, D.C., 1990
9. Schioler, L and Stiglich, J J Jr *Am. Ceram. Soc. Bull.*, 1986, 65: 289
10. Robinson, A L *Science*, 1986, 233: 25
11. Seyferth, D In: *Silicon-Based Polymer Science: A Comprehensive Resource* (Ref. 8)
12. Seyferth, D In: *Ultrastructure Processing of Advanced Ceramics*, Mackenzie, D J and Ulrich, D J (eds), Wiley, New York, 1988, Chapter 1
13. Wynne, K J In: *Inorganic and Organometallic Polymers* Zeldin, M, Wynne, K J and Allcock, H R (eds), American Chemical Society, A.C.S. Symp. Ser. No. 360, Washington, D.C., 1988, Chapter 1
14. Lipowitz, J, Rabe, J A and Carr, T M *Polym. Prepr. (A.C.S. Div. Polym. Chem.)*, 1987, 28(1): 411
15. Baney, R H *Polym. Prepr. (A.C.S., Div. Polym. Chem.*, 1984, 25(1): 2
16. Mariam, Y H and Abrahams, P *Polym. Prepr. (A.C.S., Div. Polym. Chem.*, 1988, 29(2): 364
17. Feng, K and Mariam, Y H *Polym. Mater. Sci. Eng.*, 1990, 63: 897
18. Derome, A E *Modern NMR Techniques for Chemistry Research*, Pergamon Press, New York, 1988
19. Maudsley, A A, Muller, L and Ernst, R R *J. Magn. Reson.* 1977, 28: 463
20. Bax, A and Morris, G A *J. Magn. Reson.*, 1981, 42: 501
21. Nardin, R and Vincendon, M *J. Magn. Reson.*, 1985, 61: 338
22. Bax, A *J. Magn. Reson.*, 1983, 53: 517
23. Kummer, D and Rochow, E *Inorg. Chem.*, 1965, 4: 1450
24. Abrahams, P M.S. Thesis, Atlanta University, 1988
25. Cragg, R H and Ma, C K *J. Organomet. Chem.*, 1986, 340: 87
26. Feng, K and Mariam, Y H *Macromolecules*, 1991, 24: 4729